Magnetic vortices in ultrathin films

E. Yu. Vedmedenko
Groupe de Physique des Solides, UMR 7588 - CNRS, Universités Paris 7 et Paris 6, 75251 Paris 5, France and Biophysical Department, Medical University of Lugansk, 348045 Lugansk, Ukraine

A. Ghazali*
Groupe de Physique des Solides, UMR 7588 - CNRS, Universités Paris 7 et Paris 6, 75251 Paris 5, France

J.-C. S. Lévy
Laboratoire de Physique Théorique de la Matière Condensée, Université Paris 7, case 7020, 75251 Paris 5, France

(Received 6 October 1998)

By means of Monte Carlo simulations, magnetic configurations with *vortices* are shown to appear in ultrathin magnetic films with exchange and dipolar interactions. The stability of these vortices is studied in detail. The presence of perpendicular anisotropy and external magnetic field is also investigated. A magnetic soliton is shown to appear during in-plane magnetization reversal. [S0163-1829(99)01005-X]

Recent experiments on epitaxial magnetic layers[1] have introduced a class of two-dimensional (2D) magnetic systems. Different complex domain structures with some evidence for defects have been observed in thin films and bilayer systems by means of Foucault imaging,[2,3] and in nanostructures, by magnetic force microscopy experiments.[4] Complex magnetic structures are inherent in such systems because of competitions between short-range and long-range interactions. Recent theoretical works on domain structures of vector spins in magnetic monolayers have been performed either by semianalytical calculations on conjectured configurations,[5] or by Monte Carlo simulations.[6,7] These theoretical studies provide evidence for the existence of several solutions for spin configurations. Major questions remain in such 2D complex systems: Are there uniform stable spin configurations or not, and if not, are there intrinsic topological defects and how are they organized? In order to answer these questions, numerical studies of the stability of realistic magnetic configurations with vector spins are needed. This is the aim of this paper. Spin configurations of much larger systems than those considered before[6,7] are obtained by means of extensive Monte Carlo (MC) treatments: Initial random configurations are submitted to a long annealing at a high enough temperature followed by a stepwise slow cooling down in order to obtain equilibrium spin configurations at very low temperature. Two particular configurations both with and without MC relaxation are also studied for energy comparison.

The general Hamiltonian of a monolayer lattice in the x-y plane with three-component vector spins $\mathbf{S}$ and $S=1$ includes local exchange, dipolar interactions, perpendicular anisotropy, and external field:

$$\mathcal{H}=-\sum_{\langle ij\rangle}\mathcal{J}\mathbf{S_i}\cdot\mathbf{S_j}+\mathrm{D}\sum_{\mathbf{ij}}\left(\frac{\mathbf{S_i}\cdot\mathbf{S_j}}{\mathbf{r_{ij}^3}}-\mathbf{3}\frac{(\mathbf{S_i}\cdot\mathbf{r_{ij}})(\mathbf{S_j}\cdot\mathbf{r_{ij}})}{\mathbf{r_{ij}^5}}\right)-\mathbf{A}\sum_{\mathbf{i}}\mathbf{S_{i,z}^2}-\sum_{\mathbf{i}}\mathbf{H}\cdot\mathbf{S_i}. \tag{1}$$

Here J is the exchange interaction which is assumed to be nonzero only for nearest-neighbor couplings. D is the dipolar coupling parameter and the running site subscripts i and j define the in-plane vector $\mathbf{r_{ij}}$. The parameter A measures the perpendicular single-site anisotropy energy. The external field $\mathbf{H}$ may have any direction.

Simple remarks can be deduced from a scaling approach. They enable us to consider very large samples which could not be introduced directly in the present numerical computation. Let us define the dimensionless parameter $K=D/(Ja^3)$ with the lattice parameter a. Without anisotropy and without external field, the scaling parameter a remains the only free variable: Different ratios D/J can be considered as issued from a single case with a given K value but with different effective lattice parameters a. As usual, this size scaling is valid as far as the discrete character of the lattice can be neglected. Thus increasing the dipolar coupling D while keeping the exchange coupling J constant amounts to a mere increase of the effective lattice parameter a. In the usual magnets, the ratio $D/(Ja_0^3)$ is of the order of 10^{-3}–10^{-4}, where a_0 is a typical atomic distance in metals. Thus, for $D/J=0.1$, $a\approx 5a_0$–$10a_0$ and for $D/J=1$, $a\approx 10a_0$–$20a_0$. So large values of D/J are relevant to large samples. In the present work, we used large values of D/J to consider scales much larger than a few tens of atomic distances.

In the present calculations, samples with free boundaries are considered. It is well known that dipolar contributions depend on the shape of the sample. This is the demagnetizing field effect. Without anisotropy and without external field, our final MC spin configurations at very low temperature are in-plane, in keeping with known results from magnetostatics. In addition, the boundary-layer spins are in general parallel to the sample boundary. This is in agreement with the van den Berg's geometrical approach to in-plane domain structures in 2D spin configurations.[8] We present results for disk-shaped and rectangle-shaped samples. Typical low-temperature spin morphologies obtained in this work are shown in Fig. 1 for disks of 10 192 spins on a triangular lattice with $D/J=0.1$, $D/J=1$, and $J=0$, respectively. The

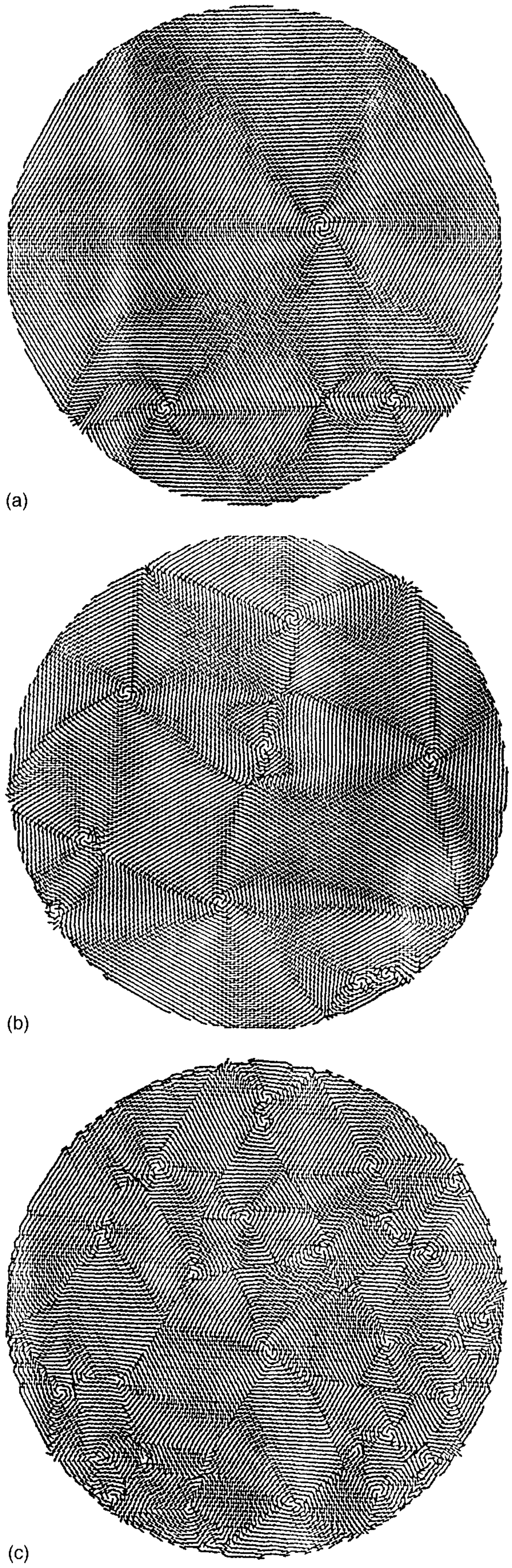

(a) (b) (c)

FIG. 1. Low-temperature spin configurations. Samples are disks of 10 192 vector spins on a triangular lattice: (a) $D/J=0.1$, (b) $D/J=1$, (c) pure dipolar coupling: $J=0$.

sample diameter covers about 106 effective spin sites. The MC calculations have been performed *without cutoff length* in the dipolar interactions. As will be discussed below, this is important because the screening of dipolar interactions due to in-plane configurations is very weak.

In the case $D/J=0.1$, i.e., at submicrometer size in a realistic material (disk diameter $\approx 500a_0$–$1000a_0$), the energies per spin obtained for the above-mentioned configurations are all quite close to each other. The ferromagnetic configuration has even a lower energy than the optimal MC configuration shown in Fig. 1 which contains only a few vortices. Thus for a sample of such a size, only one or two vortices are present in the ideal structure.

When $D/J=1$, i.e., at a larger size in a realistic material (disk diameter $\approx 1000a_0$–$2000a_0$), the ferromagnetic configuration has the highest energy among all the considered configurations. This is evidence for the stability of configurations with several vortices in the sample at such a mesoscopic size.

Finally, in the pure dipolar case, i.e., at a macroscopic scale in a realistic material, configurations obtained from MC simulations present many vortices with an energy per spin somewhat higher than the one obtained for just a single central vortex. In fact, a realistic spin configuration contains probably several vortices but less than what we found after several thousand MC steps per spin when starting from a random initial configuration. The reason for this limitation is that the single-spin MC procedure makes any vortex motion very difficult because vortices are correlated. However, expulsion of vortices is observed, generally by pairs, during a long time MC relaxation at a low temperature. Every pair expulsion is associated with a small stepwise energy drop. Thus the relaxation process is very long. This shows evidence of the strong frustration effects at all scales due to the long-range dipolar interactions.

All structures shown in Fig. 1 exhibit several *vortices*. The numbers of clockwise vortices and counterclockwise vortices are nearly equal. More precisely, one may define a local vorticity parameter as $q_i=(a/2)(\mathrm{curl}\ \mathbf{S_i})_\mathbf{z}$, with $|q_i| \leqslant 1$. This enables us to draw up the vorticity map of our samples. Figure 2 shows an example of the sign and strength of the spin field vorticity for the pure dipolar case. Spin sites with vorticity of strong absolute value define two interwoven networks of continuous lines which link the cores of vortices of the same chirality. It should be noticed that these strong vorticity lines are the domain walls. The local vorticity parameter q_i defined above provides an elegant way to find out all domain walls in a given sample. Let us mention that the strong vorticity lines are somewhat similar to von Kármán streets which link vortices of the same sign in 2D turbulent flows.[9] Such an analogy is probably connected with the strong spatial inhomogeneity of the dipolar field.

The vortex spatial distribution is analyzed by means of pair-distribution functions (PDF). When vortices of both signs are considered all together, they are distributed at random, as seen in the pictures of Fig. 1; their PDF has no significant structure. However, the PDF of vortices of a specific sign gives evidence for short-range repulsion. Thus the presence of vortices of both signs ensures a medium-range screening of the effective interaction between vortices. It must be noticed that the introduction of any cutoff length in

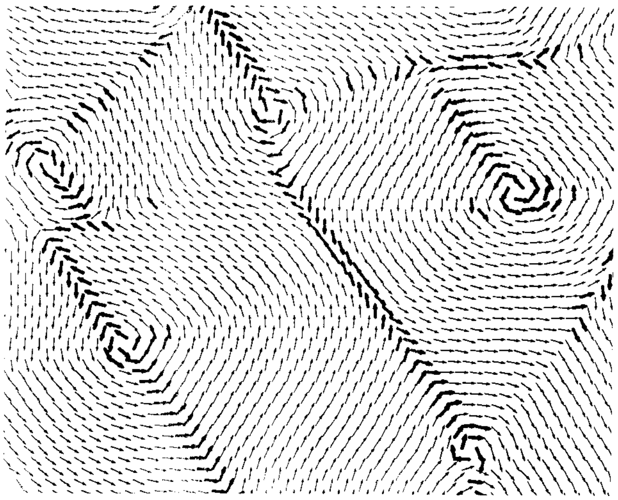

FIG. 2. Enlarged portion of Fig. 1 (c) showing domain walls defined by q_i (thick arrows). The walls connect vortices of the same sign. Here pure dipolar coupling; $k_BT/(D/a^3)=0.01$.

the dipolar interaction leads at the end of the MC thermalization process to a rather ordered vortex lattice. The lattice parameter of this lattice is approximately equal to the cutoff length. This has been checked for different cutoff lengths. It proves that the screening is very sensitive to the long-range part of the dipolar coupling. However the spin energy is only just altered by the cutoff. For instance, in a rectangle-shaped sample of 10 201 spins with pure dipolar couplings, and for cutoff lengths of 15 a and 20 a, energy differences compared to the full coupling case are found not to exceed 1%. In liquid crystals, similar ordered lattices of topological defects have been observed, as in cholesteric and smectic thin films under mechanical tension.[10] Here electric dipolar couplings play the same role as magnetic dipolar interactions in our case.[11] In liquid crystals, ion-induced screening yields a natural cutoff length and could be the reason for the appearance of such an order.

For disks of 10 192 spins on a triangular lattice, the low-temperature energies per spin for different D/J ratios are compared in Table I for (i) three MC relaxed magnetic structures derived from different initial configurations, and for (ii) two unrelaxed particular configurations. In all considered cases, the lowest energy is obtained for the configuration with a single central vortex. After a long relaxation process which ends at a very low temperature, the configuration with a single central vortex remains the one with the lowest energy among the considered configurations. This proves the stability of vortex configurations in all these cases.

TABLE I. Comparison of average energies per spin at very low temperature. Energy unit$=J$ ($=D$ for pure dipolar case).

	Energy per spin		
	$D/J=0.1$	$D/J=1$	$J=0$
MC relaxation	-3.220	-5.662	-2.701
Ideal ferro	-3.227	-5.595	-2.632
Ferro+MC	-3.223	-5.619	-2.616
1 central vortex	-3.234	-5.703	-2.743
1 vortex+MC	-3.231	-5.700	-2.740

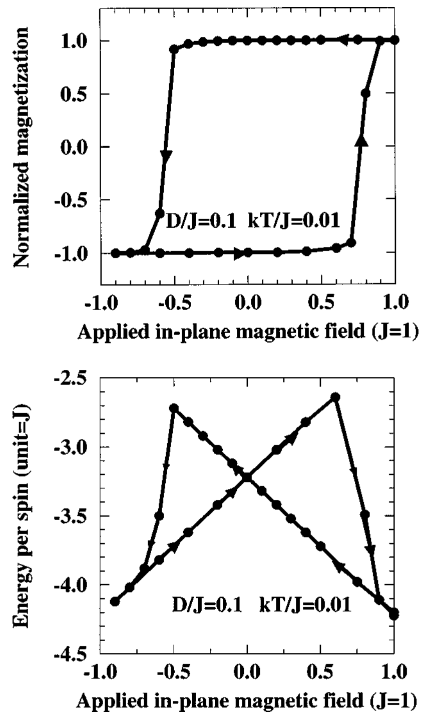

FIG. 3. In-plane field hysteresis loop: (top) magnetization, (bottom) spin energy vs applied field.

When introducing a large enough perpendicular anisotropy in the problem, all MC relaxed configurations contain many out-of-plane spins. The average value $\langle S_z^2\rangle$ is a good measure of the transition from in-plane spins towards perpendicular spins. This spin reorientation transition occurs when the uniaxial anisotropy energy is of the order of magnitude of the dipolar interaction energy. It is characterized by the appearance of several domains of twisted bunches of nearly up spins or down spins. These domains are surrounded by domains with almost in-plane spins.[12] A detailed study of the reorientation transition will be given elsewhere.[13]

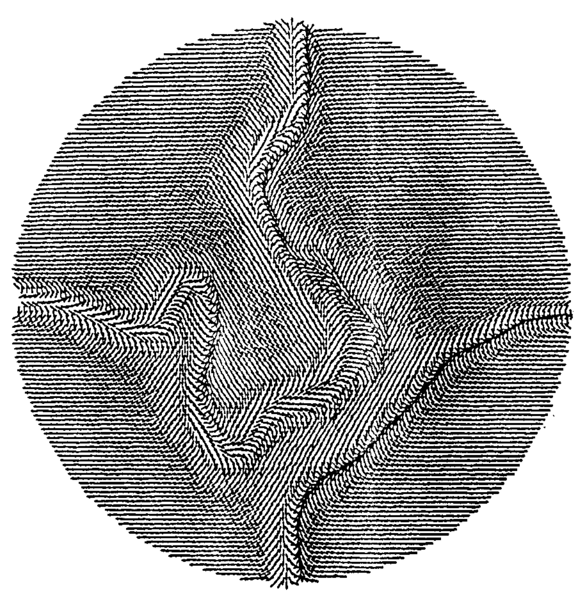

FIG. 4. Snapshot of a double-wall magnetic soliton at the in-plane coercive field. $D/J=0.1, H_x/J=-0.6, k_BT/J=0.01$.

The introduction of a high enough external field H_z normal to the surface leads also to the appearance of out-of-plane spins with a similar transition towards an Ising-type system. However, this transition occurs at a field value which is much larger than the dipolar field one.[12,13] On the contrary, the application of a moderate in-plane external field H_x is enough to saturate the in-plane magnetization. A typical rectangle-shaped magnetization *versus* applied field hysteresis loop and the respective energy *versus* field curve are reported in Fig. 3 for $D/J=0.1$. This gives evidence for a sharp quasistatic coercive field. Taking advantage of the slowness of the MC relaxation process at low temperature, we are able to show in Fig. 4 for $D/J=0.1$ a typical spin snapshot taken during magnetization reversal process. The latter occurs at a field just larger than the coercive field. The rapid propagation of the in-plane domain wall as a solitary wave, i.e., as a *soliton* with a double wall, is also evidence for strong nonlinear effects in this problem. Let us mention that some snapshots obtained in this work are very similar to those found experimentally for soft thin films; see Fig. 8 of Ref. 14.

In conclusion, let us mention that vortices were introduced as intrinsic defects in the general problem of 2D systems.[15] What we have shown here is that vortices are not only possible patterns in 2D magnetic systems with long-range dipolar interactions but that they do belong to the stable spin configurations in ultrathin films.

E.Yu.V. acknowledges financial support from the French Ministry of Education (MENESR). Part of this work was done within the framework of Contract No. CHRX-CT93-0320 of the European Economic Community.

*Author to whom correspondence should be addressed. Electronic address: ghazali@gps.jussieu.fr

[1] For a review, see R. Allenspach, J. Magn. Magn. Mater. **129**, 160 (1994).

[2] J. N. Chapman, J. Phys. D **17**, 623 (1984); A. B. Johnston, J. N. Chapman, B. Khamsehpour, and C. D. W. Wilkinson, *ibid.* **29**, 1419 (1996).

[3] A. C. Daykin and J. P. Jakubovics, J. Appl. Phys. **80**, 3408 (1996).

[4] M. Hehn, K. Ounadjela, J.-P. Bucher, F. Rousseaux, D. Decanini, B. Bartenlian, and C. Chappert, Science **272**, 1782 (1996).

[5] See, e.g., S. Prakash and C. L. Henley, Phys. Rev. B **42**, 6574 (1994).

[6] A. B. MacIsaac, K. De'Bell, and J. P. Whitehead, Phys. Rev. Lett. **80**, 616 (1998).

[7] A. Hucht and K. D. Usadel, J. Magn. Magn. Mater. **156**, 423 (1996).

[8] H. A. M. van den Berg, J. Appl. Phys. **60**, 1104 (1986).

[9] L. Prandtl and O. G. Tietjens, *Applied Hydro- and Aeromechanics* (Dover, New York, 1957), p. 130.

[10] F. Rondelez and H. Arnould, C. R. Seances Acad. Sci., Ser. B **273**, 549 (1971).

[11] For a review, see M. Seul and D. Andelman, Science **267**, 476 (1995).

[12] E. Y. Vedmedenko, A. Ghazali, and J.-C. S. Lévy, Surf. Sci. **402-404**, 391 (1998).

[13] E. Y. Vedmedenko, A. Ghazali, and J.-C. S. Lévy (unpublished).

[14] A. Hubert and M. Rührig, J. Appl. Phys. **69**, 6072 (1991).

[15] J. M. Kosterlitz and D. Thouless, J. Phys. C **6**, 1181 (1973); J. M. Kosterlitz, *ibid.* **7**, 1046 (1974).